Theoretical Studies on the Higher Oxidation States of Iron

M. Atanasov*

Institute of General and Inorganic Chemistry, Bulgarian Academy of Sciences, Bl.11, 1113 Sofia, Bulgaria, and Fachbereich Chemie und Zentrum für Materialwissenschaften der Philipps-Universität, Hans-Meerweinstrasse 1, D-35043 Marburg, Germany

Received March 5, 1999

Density functional theory (DFT) and multiconfiguration self-consistent field (MCSCF) calculations on the oxo FeO_4^{2-} (Fe^{VI}) and the hypothetical oxo FeO_4^{-} (Fe^{VII}), and FeO_4 (Fe^{VIII}) and peroxo $FeO_2(O-O)^z$ [$z = -2$ (Fe^{IV}), $z = -1$ (Fe^{V}), $z = 0$ (Fe^{VI})], $Fe(O-O)_2^z$ [$z = -2$ (Fe^{II}), $z = -1$ (Fe^{III}), $z = 0$ (Fe^{IV})], and $FeO(O-O)_2^z$ [$z = -2$ (Fe^{IV}), $z = -1$ (Fe^{V}), $z = 0$ (Fe^{VI})] clusters are presented and discussed. The results show the potential of stabilizing Fe^{VII} and Fe^{VIII} in tetrahedral oxo coordination. On the basis of absolute electronegativities calculated using DFT, it is predicted that FeO_4 will be rather oxidizing, even stronger than Cl_2 and O_2. On the basis of a comparison between total bonding energies of $M_1M_2Fe^{VI}O_4$ (M_1, M_2 = Li, K), $MFe^{VII}O_4$ (M = Li, K), and $Fe^{VI}O_4$ clusters, possible synthetic routes for electrochemical preparation of FeO_4^{-} and FeO_4 species are discussed.

I. Introduction

The stabilization of the high oxidation states of the 3d transition metals (TM) is an important problem in inorganic chemistry. Examples are the high-T_c copper(III) oxides and the materials for energy storage, such as the rechargeable Li batteries based on oxides of Ni^{III}/Ni^{IV}, Co^{III}/Co^{IV}, and Mn^{III}/Mn^{IV}.[1]

Iron in oxidation states VII (d^1) and VIII (d^0) is not known yet, despite the fact that tetrahedral tetraoxo anions of the corresponding isoelectronic V^{IV}, Cr^{V}, and Mn^{VI} (d^1) and V^{V}, Cr^{VI}, and Mn^{VII} (d^0) do exist [2] and have been thoroughly characterized by spectroscopic means.[3] On the other hand Fe^{VI} (d^2) in the red compound K_2FeO_4 has been known for a long time.

The oxidation states of TM ions in complexes can be unambiguously identified by spectroscopic methods and can be interpreted in terms of molecular orbitals (MOs) and their ground-state occupancies (electronic configuration).[4] Let us consider the metal−ligand bonding starting from an appropriately charged TM ion and the required number of anionic ligands, each in its closed shell configuration. For a d^n TM cation in tetrahedral coordination, the ground-state configuration is characterized by fully occupied bonding (a_1, e, t_2) and nonbonding (t_1, t_2) MOs and *n*-electrons in the antibonding e(π) and $t_2(\pi+\sigma)$ orbitals. While orbital contributions from 3d (TM) and ligand (L) 2p functions to the bonding and antibonding orbitals may vary in a wide range, depending on the TM−ligand covalency and ionicity, transfer of electrons from the nonbonding (L, 2p) to the antibonding t_2 and e orbitals can take place either in the ground or in the excited state and reduce by one the TM oxidation state.[5] In a recent study using charge-transfer (CT) spectra, we have been able to recognize many peculiarities of the electronic and geometric structures of the lower oxidation states of TM such as V^{IV}, Cr^{V}, and Mn^{VI} (d^1) by analyzing the ligand-to-metal charge-transfer (LMCT) spectra of the corresponding V^{V}, Cr^{VI}, and Mn^{VII} (d^0) TM tetrahedral oxo anions.[6] The electron flow from fully occupied nonbonding (ligand) MOs to empty or partly occupied antibonding orbitals is enhanced by interelectronic repulsion, which destabilizes these orbitals to a larger extent than the energetically close lying antibonding MOs. This effect is strongly counteracted by the Madelung

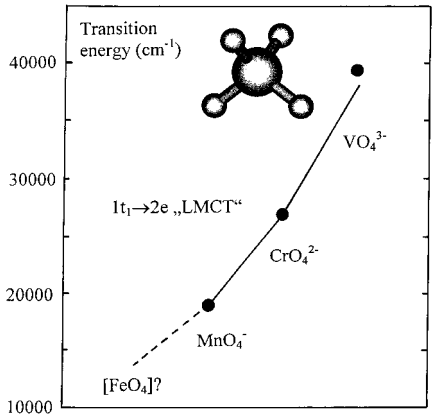

Figure 1. Lowest ($1t_1 \rightarrow 2e$) LMCT energies for the d^0 MnO_4^{-}, CrO_4^{2-} and VO_4^{3-} tetrahedral oxo anions calculated using DFT (points connected with lines) and experimental (black circles). The DFT energy of the hypothetical FeO_4 is also indicated. The plotted experimental values are taken from the following: Borromei, R.; Ingletto, G. *Chem. Phys. Lett.* **1981**, *81*, 62 (for VO_4^{3-}). Murthy, T. S. N.; Ramalingaiah,S.; Reddy, K. N.; Salagram, M. *Solid State Commun.* **1986**, *60*, 715 (for CrO_4^{2-}). Holt, S. L.; Ballhausen, C. J. *Theor. Chim. Acta* **1967**, *7*, 313 (for MnO_4^{-}).

* Address for correspondence: Fachbereich Chemie und Zentrum für Materialwissenschaften der Philipps-Universität.

(1) Pistoia, G., Ed. *Lithium Batteries*; Elsevier: Amsterdam, 1994; Industrial Library, Vol. 5.
(2) Cotton, F.A.; Wilkinson, G. *Advanced Inorganic Chemistry*, 3rd ed.; Interscience Publishers, John Wiley & Sons: New York, 1972.
(3) Brunold, T.C.; Hauser, A.; Güdel. H. U. *J. Luminesc.* **1994**, *59*, 321.
(4) Throughout this paper we use the concept of (spectroscopic) oxidation states and of preponderant electronic configurations, providing a close link between atomic spectroscopy and inorganic chemistry; see: Jørgensen, C. K. *Oxidation Numbers and Oxidation States*; Springer: New York, 1969.
(5) Atanasov, M.; Adamsky, H.; Eifert, K. *J. Solid State Chem.* **1997**, *128*, 1.
(6) Atanasov, M.; Brunold, T.C.; Güdel, H.U.; Daul, C.A. *Inorg. Chem.* **1998**, *37*, 4589.

10.1021/ic990263y CCC: $18.00
Published on Web 10/09/1999

Table 1. Total Bonding Energies (E_t, eV, Spin-Unrestricted DFT Calculations), Ground-State Spin (S), and "d^n" Configurations of FeO_4^z Oxo (O) and Peroxo (O−O) $[FeO_2(O-O)]^z$, $[Fe(O-O)_2]^z$, and $FeO(O-O)_2^z$, $z = -2, -1, 0$. Clusters at Ground-State Equilibrium Geometry

FeO_4^{2-} (Fe^{VI}, d^2)	FeO_4^{-} (Fe^{VII}, d^1)	FeO_4 (Fe^{VIII}, d^0)
$E_t(T_d) = -31.657$	$E_t(T_d) = -34.314$	$E_t(T_d) = -30.455$
$S = 1$, $2e^2$	$S = 1/2$, $2e^1$	$S = 0$, $2e^0$
$FeO_2(O-O)^{2-}$ (Fe^{IV}, d^4)	$FeO_2(O-O)^{1-}$ (Fe^{V}, d^3)	$FeO_2(O-O)$ (Fe^{VI}, d^2)
$E_t(C_{2v}) = -29.544$	$E_t(C_{2v}) = -33.548$	$E_t(C_{2v}) = -30.447$
$S = 1$, $9a_1^2 3a_2^1 10a_1^1$	$S = 1/2$, $9a_1^2 3a_2^1$	$S = 0$, $9a_1^2$
$Fe(O-O)_2^{2-}$ (Fe^{II}, d^6)	$Fe(O-O)_2^{1-}$(Fe^{III}, d^5)	$Fe(O-O)_2$ (Fe^{IV}, d^4)
$E_t(D_{2d}) = -26.665$	$E_t(D_{2d}) = -31.453$	$E_t(D_{2d}) = -28.975$
$S = 1$, $5a_1^2 5b_2^2 2b_1^1 5e^1$	$S = 1/2$, $5a_1^2 5b_2^2 2b_1^1$	$S = 0$, $5b_2^2 5a_1^2$
$FeO(O-O)_2^{2-}$ (Fe^{IV}, d^4)[a]	$FeO(O-O)_2^{-}$ (Fe^{V}, d^3)[b]	$FeO(O-O)_2$ (Fe^{VI}, d^2)[c]
$E_t(C_1) = -34.561$	$E_t(C_2) = -38.042$	$E_t(C_2) = -34.490$
$S = 0$, $23a^2 24a^2$	$S = 1/2$, $12a^2 12b^1$	$S = 0$, $12a^2$

[a] Saddle points $E_t(C_2) = -34.151$ eV, $S = 0$, $12a^2 12b^2$, $E_t(C_{2v}) = -33.871$ eV, $S = 0$; $9a_1^2 7b_2^2$. [b] Saddle points $E_t(C_{2v}) = -38.024$ eV, $S = 1/2$, $9a_1^2 7b_2^1$. [c] Saddle points $E_t(C_{2v}) = -34.394$ eV, $S = 0$, $9a_1^2$.

Table 2. Fundamental Vibrational Frequencies (cm^{-1}, DFT, Spin-Unrestricted Calculations) for Ground-State Equilibrium Geometry of Oxo (O) and Peroxo (O−O) Fe Clusters

T_d	α_1		ϵ		$\tau_2(1)$			$\tau_2(2)$	
FeO_4^{2-}	765		264		360			783	
FeO_4^{-}	840		296		395			895	
FeO_4	884		352		408			965	
C_{2v}	α_1	α_1	α_2	α_1	β_1	β_2	α_1	β_1	β_2
$FeO_2(O-O)^{2-}$	866[a]	304[a]	140[a]	537[a]	211[a]	162[a]	806[a]	752[a]	263[a]
$FeO_2(O-O)^{-}$	945	319	245	589	248	124	909	930	430
$FeO_2(O-O)$	1026	320	298	599	275	295	980	1033	574
D_{2d}	α_1	α_1	β_1	β_2	ϵ		β_2	ϵ	
$Fe(O-O)_2^{2-}$	815	399	186	524	34		826	225	
$Fe(O-O)_2^{-}$	934	508	258	692	131		948	388	
$Fe(O-O)_2$	1062	528	366	723	121		1064	530	
C_1	α								
$FeO(O-O)_2^{2-}$	128	135	180	214	253	299	361	530	637	804	844	850
C_2	α						β					
$FeO(O-O)_2^{-}$	127	198	349	560	924	942	167	208	233	335	657	898
$FeO(O-O)_2$	172	248	390	609	989	1016	52	220	251	334	642	978

[a] Result from a spin-restricted DFT calculation with a $9a_1^2 3a_2^2$ configuration.

energy, which shifts nonbonding ligand and partly occupied (or empty) orbitals apart from each other, and thus increases the LMCT energy gap.

The nearest cationic coordination of oxygen has been found to play a crucial role in stabilizing the higher oxidation states of TM in oxides and oxo anions.[7] The change in the Madelung potential via variations in the cationic coordination of oxygen (chemical constitution) leads to large changes in the redox properties of the TM. Thus, the oxidation potential of FeO_4^{2-} is considerably reduced in lattices such as K_2SO_4 and K_2CrO_4 and in concentrated (proton-withdrawing) KOH solutions; however, it increases in acidic water solutions upon formation of Fe−O−H bonds.

The variation of the cationic surrounding of oxygen leads to changes in the TM−oxygen bond and to spectacular effects in the visible and UV LMCT spectra.[7] One can conclude from the studies thus far that the lowest-energy LMCT transitions and their variation with chemical constitution can provide essential insight into the stabilization of oxidation states which are not known yet. The LMCT energies of TM tetraoxo anions shift to lower energies across the series VO_4^{3-}, CrO_4^{2-}, and MnO^{4-} (d^0) and VO_4^{4-}, CrO_4^{3-}, MnO_4^{2-} (d^1), and one may ask the question under what conditions the missing members FeO_4 (d^0) and FeO_4^{-} (d^1) might be stabilized and what properties these species are expected to display on the basis of first principle calculations. In answering this question, approximate density functional theory (DFT), which is found to reproduce experimental LMCT energies astonishingly well (Figure 1), might be helpful.

In this paper I report DFT calculations on the hypothetical FeO_4^{-} (Fe^{VII}) and FeO_4 (Fe^{VIII}) species and compare them with those of the existing FeO_4^{2-} from one side and with the corresponding mono- $[FeO_2(O-O)^z$, $z = -2$ (Fe^{IV}), $z = -1$ (Fe^{V}), $z = 0$ (Fe^{VI})] and di-peroxo $[Fe(O-O)_2^z$, $z = -2$ (Fe^{II}), $z = -1$ (Fe^{III}), $z = 0$ (Fe^{IV}) and $FeO(O-O)_2^z$, $z = -2$ (Fe^{IV}), $z = -1$ (Fe^{V}), $z = 0$ (Fe^{VI})] species from the other side. It is hoped that the results will stimulate work on the preparation and more systematic search of Fe^{VII} and Fe^{VIII} compounds.

II. Computational Details

Spin-restricted and spin-unrestricted DFT calculations have been carried out with the Amsterdam density functional (ADF) program package (version 2.3).[8−12] The Vosko−Wilk−Nusair

(7) Reinen, D.; Atanasov, M.; Lee, S.-L. *Coord. Chem. Rev.* **1998**, *175*, 91.

(8) Baerends, E. J.; Ellis, D. E.; Ros, P. *Chem. Phys.* **1973**, *2*, 41.
(9) Baerends, E. J.; Ros, P. *Int. J. Quantum Chem.* **1973**, *2*, 42.
(10) Baerends, E. J.; Ros, *P. Chem. Phys.* **1973**, *2*, 51.

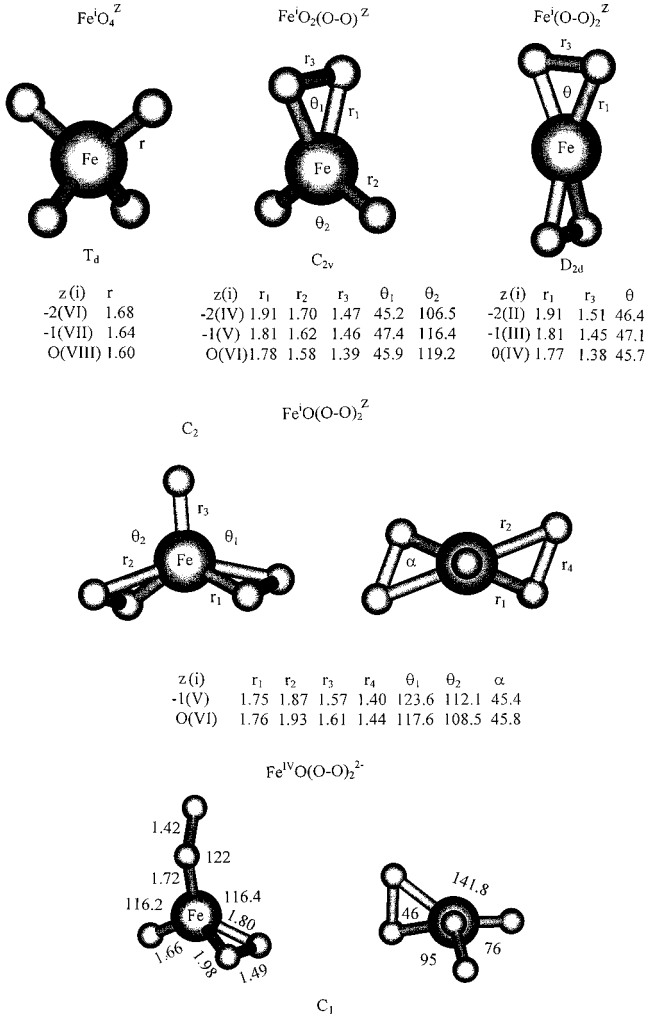

Figure 2. Cluster geometries and geometrical parameters (bond distances, Å; bond angles, (deg) of (a, top row) FeO_4^z, $FeO_2(O-O)^z$, and $Fe(O-O)_2^z$ ($z = -2, -1, 0$) and (b, bottom two rows) $FeO(O-O)_2^z$ ($z = -2, -1, 0$) iron oxo and peroxo clusters obtained from DFT geometry optimizations.

parametrization[13] of the electron gas data has been used for the exchange correlation energy and potential. Density gradient corrections were included for the exchange[14] and for the correlation.[15] Triple ς Slater type orbitals (STOs) extended by one polarization function (TZP) are used for Fe and O, where core orbitals of Fe up to 2p were kept frozen. To simulate the Madelung field and to counterbalance the excess negative charges in the case of FeO_4^- and FeO_4^{2-} clusters, four compensating charges of 0.25 and 0.5, respectively, were placed behind the metal−oxygen bonds at a distance of 1.78 Å from oxygen.

To check the reliability of the basis sets for Fe, supplied by the ADF 2.3 package and their effect on the Kohn−Sham orbital energies, spin-unrestricted ($S = 1$) calculations of the total bonding energies of FeO_4^{2-} in its ground state ($2e^2$, $^3A_2$, −50.4946 eV) and the lowest excited ligand field ($2e \rightarrow 5t_2$, −49.1358 eV) and LMCT ($1t_1 \rightarrow 2e$, −48.3031 eV) states have been performed. There is reasonable agreement between calculated (10 958 and 17 674 cm^{-1}, respectively) and experimental (12 900 and 19 000 cm^{-1} [2]) transition energies. Good agreement between calculated (using basis sets of the same quality) and experimental LMCT transition energies was also reported in μ-1,2 peroxide-bridged Fe(III) complexes.[16] In addition, the calculated ionization potential (55.74 eV) and electronic affinity (31.566 eV) of Fe^{3+} compare nicely with literature data (54.81 and 30.65 eV,[17] respectively).

Table 3. Total Energies (E_t, eV), Spin (S), Ionization Potentials (I), Electronic Affinities (A), Absolute Electronegativities [$\chi = (I + A)/2$], and Absolute Hardnesses [$\eta = (I - A)/2$] of Iron Oxo and Peroxo Clusters, of Some Strongly Oxidizing Agents (X_2 and X, X = Cl, O, F), and of $LiAsF_6$ (AsF_6^-)[a]

species	E_t (S)	I	A	χ	η
$Li_2Fe^{VI}O_4$	−39.48 (1)	8.27	0.99	4.63	3.64
$LiFe^{VII}O_4$	−35.12 (1/2)	9.75	2.65	6.20	3.55
$K_2Fe^{VI}O_4$	−37.23 (1)	5.98	0.69	3.34	2.64
$KFe^{VII}O_4$	−34.34 (1/2)	8.30	1.83	5.06	3.24
$LiKFeO_4$	−38.50 (1)	7.13	0.91	4.02	3.11
$Fe^{VIII}O_4$	−30.46 (0)	12.41	3.77	8.09	4.32
$Fe^{VI}O(O-O)_2$	−34.39 (0)	11.65	3.38	7.52	4.14
$Fe^{IV}(O-O)_2$	−28.98 (0)	9.85	2.27	6.06	3.79
Cl	−0.22 (1/2)	14.14	3.63	8.88	5.26
		(13.01)	(3.62)	(8.31)	(4.70)
Cl_2	−3.23 (0)	11.35	1.21	6.28	5.07
		(11.6)	(2.4)	(7.0)	(4.6)
O	−1.53 (1)	17.68	1.51	9.60	8.08
		(13.62)	(1.46)	(7.54)	(6.08)
O_2	−9.73 (1)	12.92	0.37	6.64	6.28
		(12.2)	(0.4)	(6.3)	(5.9)
F	−0.41 (1/2)	20.16	3.66	11.91	8.25
		(17.42)	(3.40)	(10.41)	(7.01)
F_2	−3.64(0)	15.78	0.84	8.31	7.47
AsF_6^-	−33.07(0)	7.45	−3.77	1.84	5.61
$LiAsF_6$	−33.53(0)	12.70	1.73	7.22	5.48

[a] Total energies from spin-restricted DFT calculations refer to spin-unpolarized atomic fragments. Data from experiment are given in parentheses.

For the sake of comparison, Hartree−Fock(HF) and multiconfigurational self-consistent field (MCSCF) calculations on FeO_4 have been performed using the following procedure. First using triple ς-basis and natural orbitals obtained in a simple CI calculation, a geometry optimization on FeO_4 has been performed. This has led to an Fe−O bond distance of 1.634 Å and ground-state energy of −1561.097 079 eV. In the next step a MCSCF procedure has been adopted using as active space the doubly occupied (O, 2p: $t_1 + 2t_2 + a_1 + e$) and the empty antibonding (Fe, 3d: $t_2 + e$) orbitals. A multireference CI calculation, including all single and double excitations from the reference, has been included. This has led to significant stabilization of the ground state (−1561.574 806 eV). The HF and MCSCF calculations were performed using the ab initio program GAMESS developed by Schmidt et al.[18]

III. Results and Discussion

On the basis of the total bonding energies for Fe oxo and peroxo clusters at equilibrium ground-state geometry (Table 1), one can conclude that the FeO_4^z ($z = -2, -1, 0$) clusters are more stable than the respective four-coordinate $FeO_2(O-O)^z$

(11) Boerrigter, P. M.; te Velde, G.; Baerends, E. J. *Int. J. Quantum Chem.* **1988**, *33*, 87.
(12) te Velde, G.; Baerends, E. J. *J. Comput. Phys.* **1992**, *99*, 84 and references therein.
(13) Vosko, S. H.; Wilk, L.; Nusair, N. *Can. J. Phys.* **1980**, *58*, 1200.
(14) Becke, A. D. *Phys. Rev. A* **1988**, *38*, 3098.
(15) Perdew, J. P. *Phys. Rev. B* **1986**, *33*, 8822.
(16) Brunold, T. C.; Tamura, N.; Kitajima, N.; Moro-oka, Y.; Solomon, E.I. *J. Am. Chem. Soc.* **1998**, *120*, 5674 and references therein.
(17) Parr, R. G.; Yang, W. *Density-Functional Theory of Atoms and Molecules*; Oxford University Press: New York, 1989.
(18) Schmidt, M. W.; Baldridge, K. K., Boatz, J. A.; Elbert, S. T.;Gordon, M. S.; Jensen, J. H.; Koseki, S.; Matsunaga, M.; Nguyen, K.; Su, S. J.; Windus, T. L.; Dupius, M.; Montgomery, J. A. *J. Comput. Chem.* **1993**, *14*, 1347.

Table 4. Total Bonding Energies (E_t) and Their Decomposition into Closed Shell Repulsion (E_P) Electrostatic (E_{el}) and Orbital (E_{orb}) Interaction Energies for an FeO_4 Cluster with Respect to the Free Atoms (Fe and O) and with Respect to Ionic Fragments (Fe^{8+} and O^{2-})[a]

	$E_t(FeO_4)$	E_P	E_{el}	E_{orb}	$E(a_1)$	$E(e)$	$E(t_1)$	$E(t_2)$
Fe + 4O	−30.455	68.346	−27.141	−71.660	−13.797	−1.402	−19.548	−36.883
Fe^{8+} + $4O^{2-}$	−616.822	80.012	−430.100	−266.733	−1.872	−99.912	−7.308	−156.197

[a] $E_t(FeO_4) = E_p + E_{el} + E_{orb}$. $E_{orb} = E(a_1) + E(e) + E(t_1) + E(t_2)$.

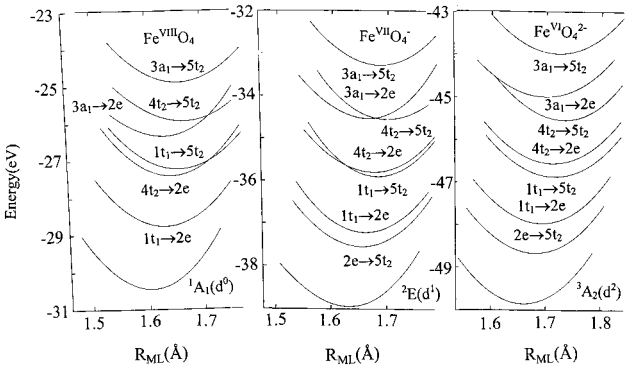

Figure 3. Total energy curves for the ground and the lowest d−d (for d^1 and d^2) and ligand-to-metal CT configurations of tetrahedral FeO_4^z [$z = 0$ (d^0), −1 (d^1), −2 (d^2)] model clusters as a function of the metal−oxygen bond distance R_{ML}.

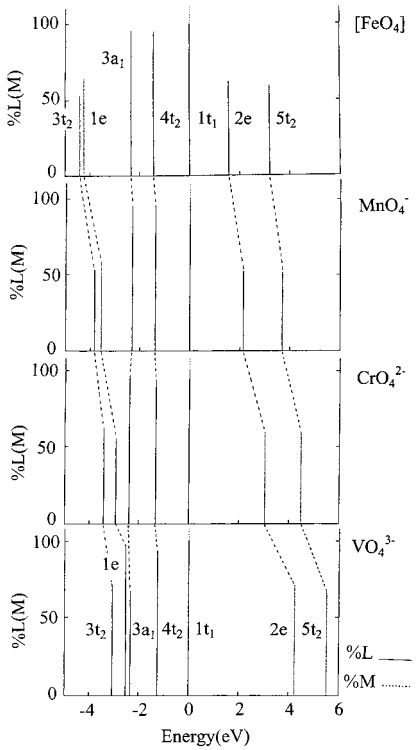

Figure 4. MO-level schemes vs O, 2p, 2s (solid lines) and M, 3d (dotted lines) orbital percentages obtained from ground-state DFT geometry optimized d^0, MO_4^z (M, z = Fe, 0; Mn, −1; Cr, −2; V, −3) clusters.

and $Fe(O-O)_2^z$ species. The difference in energy between the oxo and peroxo clusters decreases, however, with increasing Fe oxidation state from $Fe^{VI}O_4^{2-}$ to $Fe^{VII}O_4^-$ and $Fe^{VIII}O_4$. Thus, $Fe^{VIII}O_4$ and $Fe^{VI}O_2(O-O)$ are comparable in energy, FeO_4 being slightly more stable than $FeO_2(O-O)$. Ground-state equilibrium geometries for all clusters are illustrated in Figure 2. Because of the increase of the ionic radius (size) of Fe going from the higher (oxo, FeO_4^z) to the lower [peroxo, $Fe(O-O)_2^z$] oxidation states (compare the Fe−O bond lengths in Figure 2), it is expected that $Fe(O-O)_2^z$ will tend to accept one additional oxygen. DFT calculations show that $FeO(O-O)_2^z$ might be stabilized as well (cf. Table 1). Calculated vibrational energies (Table 2) show stable ground-state minima for all clusters. DFT energy diagrams including the $^1A_1(2e^0)$, $^2E(2e^1)$, and $^3A_2(2e^2)$ term energies for the Fe^{VIII}, Fe^{VII}, and Fe^{VI} tetraoxo clusters, the d−d ligand field ($2e \rightarrow 5t_2$, for d^1 and d^2), and the $1t_1 \rightarrow 2e$, $1t_1 \rightarrow 5t_2$, $4t_2 \rightarrow 2e$ and $4t_2 \rightarrow 5t_2$ CT configurations as a function of the Fe−O bond distance (R_{ML}) are presented in Figure 3.Well-developed minima with positive lowest $1t_1 \rightarrow 2e$ LMCT energies for d^0 (Fe^{VIII}), d^1 (Fe^{VII}), and d^2 (Fe^{VI}) are calculated. The DFT results predict that Fe^{VIII} and Fe^{VII} might be stabilized in tetrahedral oxo coordination, similar to $Fe^{VI}O_4^{2-}$. FeO_4 is predicted to be gaseous, while $KFeO_4$ is expected to be analogous to the well-known $KMnO_4$. However, our results indicate that FeO_4 should be strongly oxidizing. A list of values for the absolute electronegativities (χ) and hardnesses (η) of a series of Fe clusters and some strongly oxidizing agents (X_2 and X, X = Cl, O, F) are presented in Table 3. They have been calculated from the first ionization potential (I) and electronic affinity (A) using DFT and the relations [19]

$$\chi = (I + A)/2 \qquad (1)$$
$$\eta = (I - A)/2$$

On the basis of the resulting χ_{FeO_4} value (8.09 eV), we expect FeO_4 to be more strongly oxidizing than Cl_2 (χ_{Cl_2} = 6.28 eV) and O_2 (χ_{O_2} = 6.64 eV; however, compare to Cl and O). On this basis it is conceivable that FeO_4 and FeO_4^- could only be prepared by electrochemical methods (see the discussion below).

Valence orbital energies for the d^0 (FeO_4, MnO_4^-, CrO_4^{2-}, and VO_4^{3-}) oxo clusters in their $^1A_1(d^0)$ ground state obtained

Table 5. Orbital Energies (eV) and Metal Orbital Percentages (in Parentheses) of d^0 MO_4^z (M,z = V, 3−; Cr, −2; Mn, −1) Tetrahedral Oxo Anions and the Hypothetical FeO_4 from Geometry OptimizEd DFT Calculations for the $^1A_1$ Ground State[a]

orbital (occupancy)	FeO_4 energy (% M)	MnO_4^- energy (% M)	CrO_4^{2-} energy (% M)	VO_4^{3-} energy (% M)
$5t_2$ (0)	−5.585 (41)	−2.993 (49)	0.363 (58)	3.719 (67)
2e (0)	−7.207 (38)	−4.523 (48)	−1.082 (59)	2.452 (71)
$1t_1$ (6)	−8.778 (0)	−6.679 (0)	−4.109 (0)	−1.789 (0)
$4t_2$ (6)	−10.232 (5)	−8.060 (5)	−5.445 (6)	−3.030 (7)
$3a_1$ (2)	−11.126 (4)	−8.978 (5)	−6.502 (3)	−4.304 (3)
1e (4)	−13.011 (64)	−10.248 (57)	−7.041 (45)	−4.135 (33)
$3t_2$ (6)	−13.172 (53)	−10.509 (47)	−7.538 (38)	−4.874 (29)

[a] Orbital energies for MnO_4^-, CrO_4^{2-}, and VO_4^{3-} are calculated using compensating positive charges, 0.25, 0.5, and 0.75, respectively (see ref 6).

Table 6. MO Energy (eV) Levels of the Free O_2^{2-} Peroxo Anion and of Their Change (Their Average Energy e and Splitting Δe Due to O−O and Fe−O Interactions) on Coordination in $Fe(O-O)_2$

	$1\sigma_g$	$1\sigma_u$	$2\sigma_g$	$1\pi_u$	$1\pi_g$
$e(O_2^{2-})$	−8.4	−0.3	7.5	8.6	13.4
$e[Fe(O-O)_2]$	−30.0	−0.9	−12.9	−12.0	−6.8
$\Delta e[Fe(O-O)_2]$	0.5	0.0	0.1	0.2	3.5

(19) Pearson, R.G. *Inorg. Chem.* **1988**, *27*, 734.

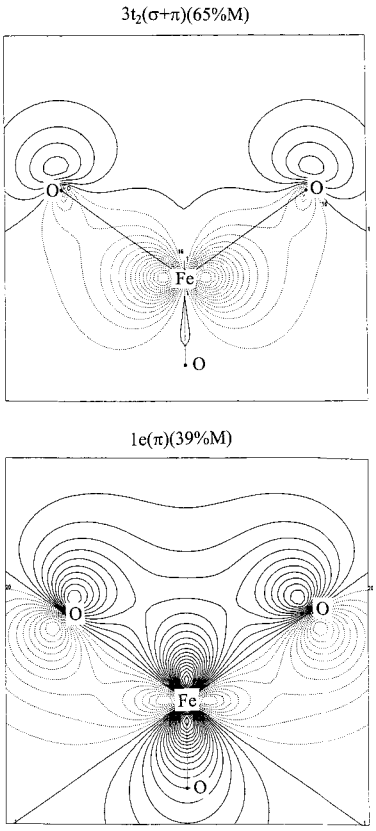

Figure 5. Contour plot diagrams for the bonding $3t_2(\sigma+\pi)$ and $1e(\pi)$ natural orbitals as obtained for the FeO_4 (hypothetical) $^1A_1$ ground-state MCSCF calculation.

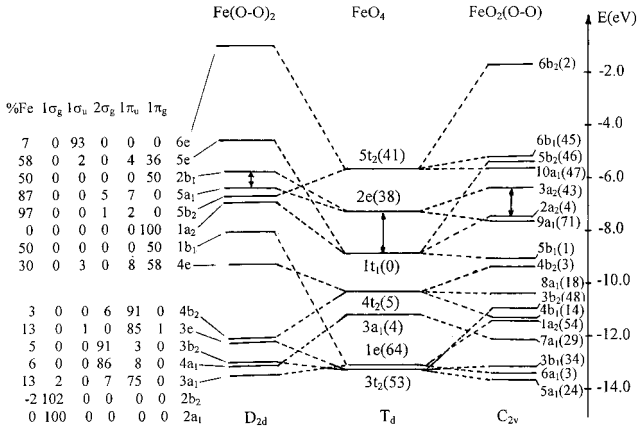

Figure 6. Energy diagram showing the correlation between DFT MOs of the hypothetical peroxo $Fe(O-O)_2$ and $FeO_2(O-O)$ and the oxo FeO_4 clusters. The percentages of the Fe (3d) orbitals only [for FeO_4 and $FeO_2(O-O)$] are given in parentheses, while percentages of both Fe(3d) and the free O_2^{2-} MOs are given for $Fe(O-O)_2$. The energy separation between the HOMO and the LUMO is indicated by a vertical double-headed arrow.

from DFT calculations along with their metal (3d) and oxygen (2s, 2p) percentages are plotted in Figure 4. The MO schemes obtained represent the well-known pattern for TM ions in tetrahedral coordination with the typical level ordering

$$3t_2 < 1e < 3a_1 < 4t_2 < 1t_1 < 2e < 5t_2 \qquad (2)$$

The $4t_2$ and $1t_1$ are approximately and strictly M−O nonbonding, and the same is also valid for the $3a_1$ orbital, reflecting negligible (4s) contributions to the M−O bonding. As seen from the contributions from Fe and O to the e and t_2 orbitals, M−O covalency is solely due to $1e(\pi)$ and $3t_2(\sigma+\pi)$ bonding orbitals. We analyzed the total bonding energy in terms of an energy decomposition into Pauli (closed shell) repulsion (E_P), electrostatic (E_{el}), and covalent (orbital, E_{orb}) bonding energies.[20,21] The components of the total bonding energy for an FeO_4 cluster calculated with respect to atomic fragments (Fe and O) and with respect to Fe^{8+} and O^{2-} ions are listed in Table 4. The latter choice, i.e., taking O^{2-} closed shell instead of atomic fragments, allows O−O interactions to be excluded from the E_{orb} energy and thus pure Fe−O covalent bonding to be studied. The results show again that interactions between Fe (3d) and O (2s, 2p) orbitals of e and t_2 symmetry dominate in E_{orb}. The comparison between two sets of calculations shows, however, that O−O coupling is rather significant. As is seen from Table 5 and Figure 4, the bonding 1e and $3t_2$ orbitals are dominated by ligand functions for VO_4^{3-} and CrO_4^{2-}, but by Fe 3d orbitals in FeO_4, showing that with increasing formal charge the metal 3d orbitals become lower in energy than the oxygen 2p orbitals. This results in an inverted bonding scheme for FeO_4 but still an appreciable mixing between the Fe (3d) and O (2s,2p) orbitals. Thus, the stabilizing factor in the case of FeO_4 is the pronounced reduction of the cationic charge by electron donation for oxygen. Unlike the more ionic VO_4^{3-} and CrO_4^{2-}, oxygen atoms in FeO_4^{1-} and FeO_4 are involved in a stronger covalent bonding to the TM. An inverted bonding scheme is reflected also by the orbital contour plot diagram for the $3t_2$ orbital obtained by our MCSCF calculations (Figure 5), which shows an admixture of ligand functions to $3t_2$ of 35% [but note the much higher ligand contribution (61%) to 1e].

A MO energy diagram giving the correlation between the MOs of FeO_4 with those of $FeO_2(O-O)$ and $Fe(O-O)_2$ (Figure

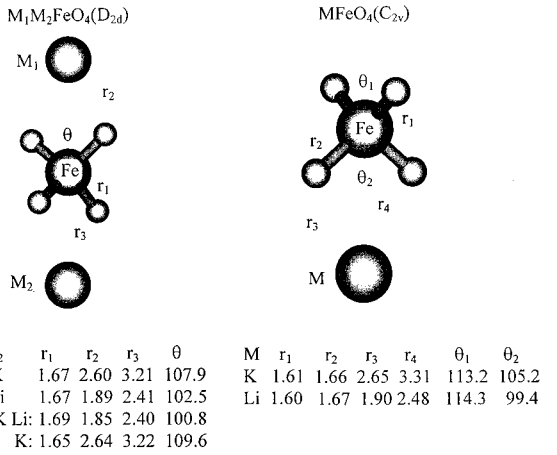

M_1	M_2	r_1	r_2	r_3	θ
K	K	1.67	2.60	3.21	107.9
Li	Li	1.67	1.89	2.41	102.5
Li	K	Li: 1.69	1.85	2.40	100.8
		K: 1.65	2.64	3.22	109.6

M	r_1	r_2	r_3	r_4	θ_1	θ_2
K	1.61	1.66	2.65	3.31	113.2	105.2
Li	1.60	1.67	1.90	2.48	114.3	99.4

Figure 7. Geometries and geometrical parameters (bond distances, Å; bond angles, deg) of $M_1M_2Fe^{VI}O_4$ (M_1, M_2 = Li, K) and $MFe^{VII}O_4$ (M = Li, K) clusters obtained from DFT geometry optimizations.

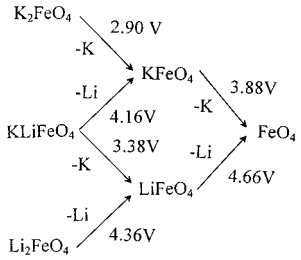

Figure 8. Voltage parameters for electrochemical oxidation of Fe in $M_1M_2Fe^{VI}O_4$ (M_1, M_2 = Li, K) to $MFe^{VII}O_4$ (M = Li, K) and FeO_4 resulting from cluster DFT calculations.

(20) Ziegler, T.; Rauk, A. *Theor. Chim. Acta (Berlin)* **1977**, *46*, 1.
(21) Ziegler, T.; Rauk, A. *Inorg. Chem.* **1979**, *18*, 1558, 1755.

Table 7. Ground-State and Lowest Excited-State Energies (ΔE, cm^{-1}), Equilibrium Fe−O Bond Distances (R_{MO}, Å) and Vibrational Energies for the Fe−O Breathing Mode ($h\nu$, cm^{-1}) in FeO_4^z ($z = 0, -1, -2$) Tetrahedral Oxo Clusters

	FeO_4			FeO_4^{1-}			FeO_4^{2-}		
state (configuration)	ΔE	R_{MO}	$h\nu_{\alpha 1}$	ΔE	R_{MO}	$h\nu_{\alpha 1}$	ΔE	R_{MO}	$h\nu_{\alpha 1}$
ground state	0	1.604	884	0	1.640	840	0	1.680	765
$2e \rightarrow 5t_2$				11 543	1.654	784	9 756	1.681	769
$1t_1 \rightarrow 2e$	13 920	1.630	836	14 434	1.660	807	15 754	1.693	765
$1t_1 \rightarrow 5t_2$	27 489	1.656	792	26 190	1.682	835	25 573	1.715	731
$4t_2 \rightarrow 2e$	25 452	1.643	849	26 351	1.675	758	27 939	1.712	731
$4t_2 \rightarrow 5t_2$	38 277	1.667	738	37 924	1.698	753	37 605	1.733	765
$3a_1 \rightarrow 2e$	33439	1.630	794	36 212	1.664	797	39 860	1.699	686
$3a_1 \rightarrow 5t_2$	46 287	1.657	769	47 216	1.686	759	49 233	1.723	714

6) shows that the ground state of FeO_4 correlates with an electronically 2-fold [$1t_1^6 2e^0$ (FeO_4) → $1t_1^4 2e^2$ ($FeO_2(O-O)$)] and 4-fold [$1t_1^6 2e^0 5t_2^0$ (FeO_4) → $1t_1^2 2e^2 5t_2^2$($Fe(O-O)_2$)] excited state going to $FeO_2(O-O)$ and $Fe(O-O)_2$, respectively. It follows that an interconversion from FeO_4 to $FeO_2(O-O)$ and $Fe(O-O)_2$ and vice versa is electronically strongly forbidden; it can proceed neither photochemically nor by thermal activation. However, this may change for O−O when two metal centers are bridged. It seems that, once formed, single-nucleous four-coordinate iron peroxides will be stabilized kinetically against further transformation to the thermodynamically more stable oxide species and they will further tend to increase their coordination number, forming $FeO(O-O)_2^z$ species ($z = -1,0$, but compare to $z = -2$, Figure 2b and Table 1). Very probably peroxo species are formed (besides K_2FeO_4) when using KNO_3/KOH melts with an excess of KNO_3,[22] e.g.

$$Fe_2O_3 + 5KNO_3 + 4KOH \rightarrow 2K_2FeO_5 + 5KNO_2 + 2H_2O \quad (3)$$

The geometry of the $FeO(O-O)_2^{2-}$ cluster deduced by our DFT calculation (Figure 2b) serves as a candidate for the coordination of Fe in the green K_2FeO_5 compound, whose structure is not known yet. Metal−peroxo bonds play a central role in the function of a variety of metalloenzymes.[16] As follows by our calculations, the main contributions to the covalency of the Fe−peroxo bond originate from the $1\pi_g$ antibonding MOs of the O_2^{2-} ligand and include σ- and π-bonding interactions between these orbitals and the Fe (3d) orbitals of t_2 symmetry (T_d). This is nicely illustrated by Figure 6 and Table 6 which compares the energy levels of one separate O_2^{2-} unit with the corresponding MOs in $Fe(O-O)_2$. The MOs of the two coordinating O_2^{2-} groups shift and split in $Fe(O-O)_2$ due to Fe−O and O−O interactions.

A comparison of DFT energies for various configurations, equilibrium bond lengths, and Fe−O breathing mode vibrational energies for FeO_4, FeO_4^- and FeO_4^{2-} (Table 7) shows that the lowest $1t_1 \rightarrow 1e$ LMCT energy increases in the sequence FeO_4, FeO_4^-, and FeO_4^{2-} (13 920, 14 434, and 15 754 cm^{-1}). Lowest LMCT energies seem to be considerably overestimated at the MCSCF level, however (compare the 13 920 cm^{-1} energy for FeO_4 with the MCSCF value, 58 220 cm^{-1}). The increase of equilibrium bond lengths upon $1t_1 \rightarrow 2e,5t_2$ excitation reflects the weakening of the Fe−O bond due to the extra electron in the antibonding $2e(\pi)$ and $5t_2(\sigma+\pi)$ orbitals, the effect being more pronounced for the $\sigma+\pi$-type $5t_2$ compared to the π-type 2e orbital.

On the basis of the calculated χ values of FeO_4^- and FeO_4 (Table 3), we expect that electrochemical extraction of alkaline metals from Fe^{VI} solids such as Li_2FeO_4, $KLiFeO_4$, and K_2FeO_4 is the only method which may probably lead to Fe in oxidation states VII and VIII.[23]

A rough estimate of the voltages of electrochemical cells needed to deintercalate the alkaline metal is possible on the basis of DFT calculations of $M_1M_2FeO_4$ (M_1, M_2 = Li, K) and $MFeO_4$ (M = Li, K) model clusters. Adopted cluster geometries and geometrical parameters from DFT geometry optimizations are depicted in Figure 7. From a comparison of the total bonding energies and their changes from $M_1M_2Fe^{VI}O_4$ to $MFe^{VII}O_4$ and $Fe^{VIII}O_4$, average electrochemical cell voltages for a consecutive extraction of one and two alkaline metals are calculated (Figure 8). Before one tries to apply these results to real systems, one should keep in mind that the cluster DFT calculations (Figure 8) neglect the crystal Madelung potential and the actual lattice topology. Moreover, if one considers conventional Li-coin-type cells, composed of oxide cathodes and a Li sheet as an anode, calculated voltages (Figure 8) have to be reduced by the cohesion energies of metallic Li and K [Li (1.22 eV), K (0.5 eV) [24]]. As follows from Figure 8, the cell voltage is expected to decrease from K to Li and from $Fe^{IV} \rightarrow Fe^{VII}$ to $Fe^{VII} \rightarrow Fe^{VIII}$ oxidations of Fe.[25]

IV. Conclusions

(1) On the basis of the DFT results, one can conclude that Fe^{VII} and Fe^{VIII} might be stabilized in tetrahedral oxo coordination, a result of strong Fe−O covalency. The energetic stabilization of the d orbitals, yielding main contributions to bonding MOs, leads to small effective metal charges and to shifting of the metal 3d orbitals from the antibonding to the bonding energy region (inverted bonding scheme) with a still appreciable amount of covalent mixing between Fe (3d) and O (2s,2p) orbitals, however. Clearly, the stabilization of higher oxidation states of the TM by this mechanism will increase as metal 3d orbitals get deeper in energy from left to right of the transition series and on going from more to less electronegative ligands. A good example is Cu^{III} in the stable square planar complex $Cu(dtc)_2^+$ (dtc = dithiocarbamate), which is easily obtainable under mild

(22) *Gmelin Handbook of Inorganic Chemistry*, 8th ed.; Berlin-Verlag Chemie: Weinheim/Bergstr. und Berlin, 1932; Volume Iron B, p 916 and references therein (in German).

(23) See for example: Nishijima, M.; Takeda, Y.; Imanishi, N.; Yamamoto, O.J. *Solid State Chem.* **1994**, *113*, 205.

(24) *Gmelin Handbook of Inorganic Chemistry*, 8th ed.; Berlin-Verlag Chemie: Weinheim/Bergstr. und Berlin, 1927; Volume Lithium, p 33; 1936; Volume Kalium, p 94. (in German).

(25) A high ionization potential and low electronic affinity of the electrolyte will guarantee that no processes, such as oxidation of electrolyte anions, will concur with the electrochemical extraction of Li. According to our DFT calculation (see Table 3) a good candidate would be $LiAsF_6$ in 2-methyltetrahydrofuran. Host lattices of the phenacite type such as Li_2CrO_4 and Li_2WO_4 (see: Muller, O.; Roy, R. *The Major Ternary Structural Families*; Springer-Verlag: Berlin, Heidelberg, New York, 1974; pp 38−39) doped with Fe^{VI} are expected to provide a good interstitial network for diffusion of Li, assuming there is a way of providing electronic mobilities in these insulating oxides.

oxidation conditions from the corresponding neutral Cu^{II} complex.[26] The same trend is also expected when the oxidation state of a given TM is increased, since the metal 3d energy decreases with increasing formal charge. In this respect, Fe^{VII} and Fe^{VIII} valence forms are good candidates for such a type of stabilization. However, the further lowering of the energies of the 3d orbitals on going to the heavier TM, Co, Ni ,Cu, and Zn will tend to draw them, in extreme cases such as these, into the electronic core and thus make them not readily available for bonding. A calculation on the series of hypothetical isovalent $M^{VIII}O_4$ species (M = Fe, Co, Ni, Cu, Zn) shows indeed that along the series Fe, Co, Ni, Cu, and Zn metal−ligand bonding becomes strongly reduced.[27]

(2) The calculated high oxidation potentials for the hypothetical FeO_4 and FeO_4^- clusters and the possibility that using KNO_3/KOH as oxidation agent, metastable species containing Fe−peroxo bonds, rather than Fe^{VII} and Fe^{VIII} oxo anions, will be formed lead one to expect that electrochemical extraction of alkaline metals from iron(VI) oxides would be the only method which may lead to Fe in oxidation states VII and VIII.

Acknowledgment. This work has been performed with the aid of a grant from the Swiss Federal Office of Energy (Swiss lithium battery project). The author is grateful to Prof. Dr. C. Daul for hospitality and the possibility to use the ADF 2.3 program code. Stimulating discussions with Prof. Dr. M. Jansen, MPI für Festkörperforschung, Stuttgart, Germany, are gratefully acknowledged. I owe thanks to one reviewer for careful reading of the manuscript and helpful criticism.

IC990263Y

(26) Willemse, J.; Cras, J. A.; Steggerda, J.J.; Keijzers, C.P. *Struct. Bonding (Berlin)* **1976**, *28*, 83−126.

(27) Total bonding energies (E_t) for the hypothetical CoO_4, NiO_4, CuO_4, and ZnO_4 clusters (equilibrium T_d geometry, basis sets as specified in section II) are, respectively, −26 .4736($2e^1$), −22.1830 ($2e^2$), −14.8603 ($2e^3$), and −11.4378 ($2e^4$) eV (compare with $E_t(FeO_4)$ = −30.4549 eV, all bonding energies calculated with respect to the respective free atomic fragments). Calculated M−O equilibrium bond distances are 1.604, 1.624, 1.657, 1.707, and 1.804 Å for Fe, Co, Ni, Cu, and Zn. They reflect the weakening of the M−O bond across the series from Fe to Zn.